Nano Energy 39 (2017) 328–336

Contents lists available at ScienceDirect

Nano Energy

journal homepage: www.elsevier.com/locate/nanoen

Full paper

An ultrathin paper-based self-powered system for portable electronics and wireless human-machine interaction

Xu He[a,b,1], Yunlong Zi[a,1], Hua Yu[a,c,1], Steven L. Zhang[a], Jie Wang[a,d], Wenbo Ding[a], Haiyang Zou[a], Wei Zhang[b], Canhui Lu[b], Zhong Lin Wang[a,d,*]

[a] School of Materials Science and Engineering, Georgia Institute of Technology, Atlanta, GA 30332, United States
[b] State Key Laboratory of Polymer Materials Engineering, Polymer Research Institute at Sichuan University, Chengdu 610065, China
[c] Key Laboratory for Optoelectronic Technology & Systems, Ministry of Education of China, key Laboratory of Fundamental Science of Micro/Nano-Device and System Technology, Chongqing University, Chongqing 400044, China
[d] Beijing Institute of Nanoenergy and Nanosystems, Chinese Academy of Sciences, National Center for Nanoscience and Technology (NCNST), Beijing 100083, China

ARTICLE INFO

Keywords:
Triboelectrical nanogenerators
Paper based electronics
Supercapacitors
Touch sensors
Wireless management

ABSTRACT

Developing lightweight, flexible and sustainable sensor networks with miniaturized integration and functionality for the Internet of Things (IoT) remains a challenge and an urgent demand for the next-generation electronic devices. Paper-based electronics, which represents one of the main green electronics in the future, have been considered as one of the most exciting technologies to meet the consumption of the frequently upgraded electronics. Here, we presented an ultrathin (about 200 μm) and lightweight paper-based self-powered system that consists of a paper-based triboelectric/piezoelectric hybrid nanogenerator and a paper-based supercapacitor. Under human motions such as flipping the page and moving the book/document, the as-fabricated self-powered system built-in the smart book/document was capable of sustaining power for portable devices, such as continuously driving LEDs and the temperature/humidity sensor. With the signal-processing circuit, the paper-based system was further developed into a wireless human-machine interaction system for documents management and smart reading. The ultrathin and highly flexible characteristics of the self-powered system not only endow the device with power generation feature for portable devices, but also build up the wireless human-machine interactions in developing potential applications for the IoT.

1. Introduction

The Internet of Things (IoT), which aims to realize the information exchange and communications of any things with the internet, needs large-scale sensor networks and systems for health monitoring, environmental protection, infrastructure monitoring and security, and has been a key driving force for the fast development of the industry and information technology [1,2]. Although the power for driving each sensor is small, which could be down to micro-watt level, the number of these units is usually huge in the order of billions to trillions [2]. Batteries, the most conventional technology for the IoT, may not be the solution due to the wide distribution of the sensor networks, limited lifetime, and difficulties in replacing/recycling. The IoT would be impossible without making the devices self-powered. Therefore, it is desirable to integrate an energy harvester together with a battery or capacitor to form a self-powered system for sustainably driving these devices [1,2]. Nanogenerators [3], as based on the mechanism of piezoelectric [4], triboelectric [5], and pyroelectric effects [6], have been developed to drive electronic devices continuously through harvesting ubiquitous energy from ambient environment. Amidst the nanogenerators, triboelectric nanogenerator (TENG) [2,5,7] is a newly invented renewable technology that has attracted significant attention, due to the high energy conversion efficiency, low-cost, and environmental friendly features. Given the nature of the pulsed output generated by the TENG, miniaturized supercapacitor is a good choice for developing the self-powered system with TENGs due to advantages of ultrafast charging and discharging rates, high power density, long life cycles and environmental benignancy [8–11].

In the past few years, lightweight and transparent TENGs received a booming time as the transparent and flexible functionality and portability endow the TENG with possibility for new applications. Fan and his coworkers [12] firstly developed a new flexible transparent nano-

* Corresponding author at: School of Materials Science and Engineering, Georgia Institute of Technology, Atlanta, GA 30332-0245, United States.
E-mail address: zhong.wang@mse.gatech.edu (Z.L. Wang).
[1] These authors contributed equally to this work.

http://dx.doi.org/10.1016/j.nanoen.2017.06.046
Received 24 April 2017; Received in revised form 25 June 2017; Accepted 27 June 2017
Available online 28 June 2017

generator based on the triboelectric process and demonstrated its potential applications for touchscreens, electronic displays, and even personal electronics. Kim et al. [13] have successfully demonstrated the application of CVD-grown graphene as a transparent, flexible TENG for powering an LCD, LEDs, and an EL display without any external energy source. More recently, Luo et al. [14] reported a transparent and flexible self-charging power film which functions either as a power generator or as a self-powered information input matrix for touch screen security applications. On the other hand, the rapidly increasing consumption of the frequently upgraded electronics has inspired the study of electronic systems which consists of renewable and biodegradable materials and minimal amount of potentially toxic materials, [15]. Paper, as formed by multiple layers of cellulose fibers and recognized as the most environmental-friendly, renewable and worldwide abundant material [16], has been intensively studied in the past two decades, and gratifying advancement of paper electronics has been witnessed [17–19]. Paper electronics have been considered as one of the most exciting technologies in the near future due to its sustainability, low cost, mechanical flexibility [20]. Recently, paper-based energy harvester have been intensively developed for self-powered generation and self-powered sensing [21–25]. However, they are neither lightweight self-powered system nor with transparency, which represents one of the main limitations for a number of applications in miniaturized electronics. Besides, the most frequently applications of paper in our life, such as books, documents and packages, are neglected. As there is no work on transparent energy harvester which combines the self-powered generation/sensing with books or documents and without sacrificing the readability, flexibility and lightweight of the paper.

Herein, we presented an ultrathin and lightweight paper-based self-powered system which consists of a paper-based triboelectric/piezoelectric hybrid nanogenerator (PHNG) and a paper-based supercapacitor (PSC). Through the bottom-up method and electrospinning technology, a transparent piezoelectric nanogenerator (PENG) was integrated in the paper-based TENG with a greatly reduced thickness, without sacrificing common features of the paper, such as readability and flexibility. The PHNG can be easily assembled with a thin paper-based supercapacitor (PSC) in books or documents as a self-powered system, serving as a power source for portable devices. The paper-based self-powered system was further developed into a wireless sensing system triggered by finger/paper touch motions. Through the signal-processing circuit, the generated electrical signal induced by human motions can operate the remote controller and the infrared sensor in a simple way, which ensures an electrical signal recognition process allowed for intriguing applications such as documents management and smart reading. These ultrathin and highly flexible characteristics of the self-powered system not only endow the device with power generation feature for portable devices, but also build up the bridge between human and machine through wireless interactions towards the IoT.

2. Results and discussion

2.1. Main idea of the self-powered system

The main idea for the design is to fabricate a transparent, ultrathin and flexible PHNG on paper with a PSC to form a self-powered system, so that both energy harvesting and self-powered sensing can be realized simultaneously during reading. As illustrated in Fig. 1, the mechanical energy triggered from human motions was harvested and converted to electricity by an ultrathin PHNG and then stored in a thin PSC for driving portable electronics continuously. On the other hand, the self-powered system can also be developed as a self-powered sensor in the wireless human-machine interaction system realized by finger/paper touch, allowing for practical applications such as documents management and smart reading.

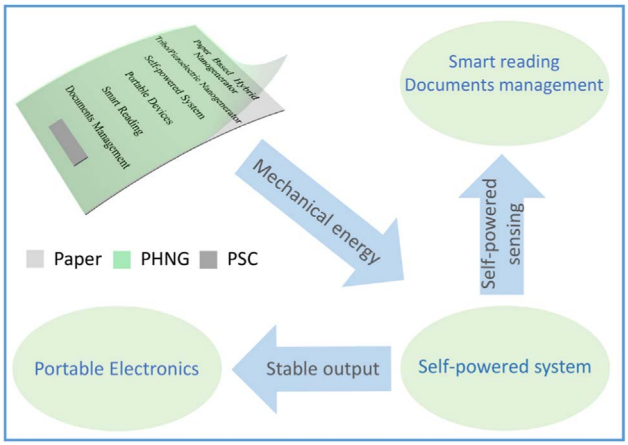

Fig. 1. Design of the self-powered system for portable electronics and self-powered sensing. Mechanical energy from human motions can be harvested and converted to electricity by the PHNG and then stored into a PSC for sustainably driving portable electronics and self-powered sensing. The schematic illustration of the paper-based self-powered system is shown in top-left.

2.2. Structure design of the PHNG

The fabrication process and multilayer structure of the proposed PHNG is schematically illustrated in Fig. 2a and b, respectively. In consideration of fabricating a thin energy harvester on a common paper, we adopted the bottom-up method and electrospinning technique. Electrospun poly(vinylidene fluoride) (PVDF) nanofibers membrane was chosen as the material for piezoelectric nanogenerator, which is ultrathin, flexible, and lightweight. The strong piezoelectricity without any stretching and poling treatment has been demonstrated for this membrane [26,27]. Right-down insert in Fig. 2b shows the SEM image of nanostructures in electrospun PVDF membrane. Due to the unique nanostructures of the electrospun nanofibers membrane, the non-transparent PVDF nanofibers membrane can be easily assembled with PDMS to form a transparent composite membrane. The total transmittance was measured with a UV–vis spectrometer using a blank substrate as the reference. The composite film shows a high total transmission of over a wavelength in the visible and near-IR ranges (400–1000 nm) as shown in Fig. S1a. To better show the transparency effect, the photographs of the transparent composite membrane and bare electrospun PVDF nanofibers were compared and shown in Fig. S1b. The high transmission value (89.7% @ 1000 nm) achieved here is attributed to the light reflectance effect of the unique nano/micro porous networks of the electrospun PVDF nanofibers when penetrated by the transparent PDMS. The SEM image (Fig. S1c) illustrates a porous nano/micro-structure in the electrospun PVDF nanofibers membrane. Finally, a thin ITO deposited fluorinated ethylene propylene (FEP) was assembled on top with an ITO layer as a shared electrode for both TENG and PENG. To increase the triboelectrification effect and further enhance the output performance of the TENG, a high surface area was achieved by fabricating nanowire array structures on the surface of the FEP film via inductively coupled plasma (ICP) reactive-ion etching [28]. Right-up insert in Fig. 2b shows the SEM image of the nanostructures on FEP. As shown in Fig. 2c, the number '2' wrote on the paper can be clearly seen with the assembly of the PHNG on top, ensuring a good readability. Fig. 2d shows the highly bent state of the PHNG, indicating a good flexibility that is mainly attributed to the ultrathin and unique nano/micro-structure of our PHNG. Owing to the bottom-up method and electrospinning technique, the thickness of the PHNG is measured at only 174 μm and stays on the same level with that of a copy paper (Fig. 2e), which ensures an excellent flexibility of the PHNG. It could be further developed as a miniaturized device for potential applications in the IoT.

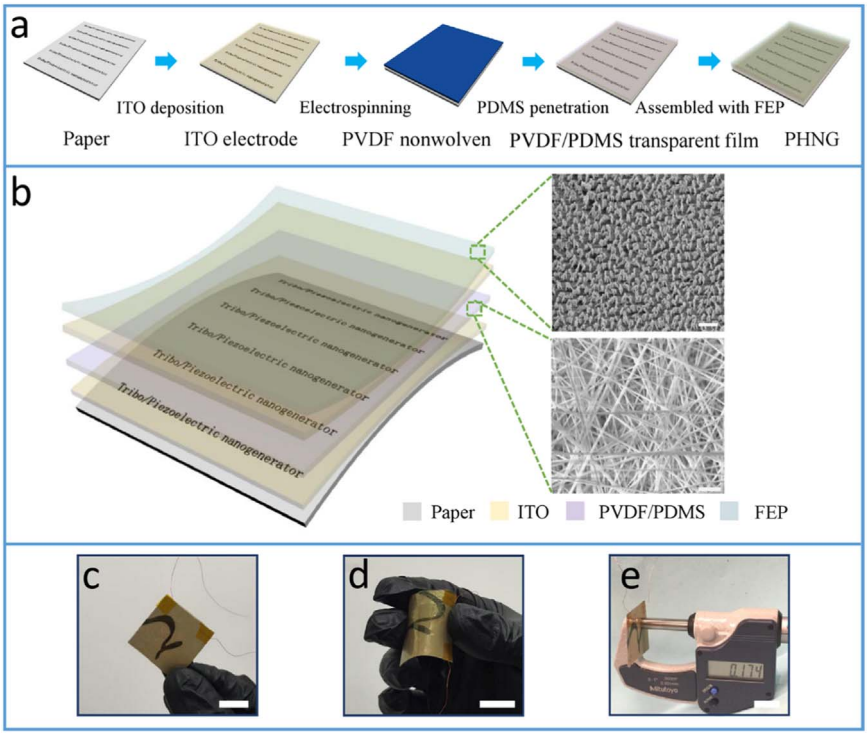

Fig. 2. Fabrication process and schematic of PHNG. (**a**) Fabrication process of the PHNG. (**b**) Schematic structure of the PHNG. Right-up and Right-down inserts show the SEM image of the nanostructure on FEP and electrospun PVDF nanofibers membrane. Scale bar: 1 μm. The photographs of the PHNG, (**c**) the number '2' wrote on paper can be clearly seen after assembled with the PHNG, (**d**) bent state of the PHNG, (**e**) the thickness of the PHNG is at the same level with that of a copy paper. Scale bar: 10 mm.

2.3. Working mechanism and electrical outputs of the PHNG

The working mechanism of the PHNG for electrical signal generation triggered by human motions could be elucidated as two parts, namely, the TENG based on the coupling of triboelectrification and electrostatic induction [2], and the PENG based on the piezoelectric effect [29]. In the TENG part, Fig. 1a shows the working mechanism of TENG for energy harvesting, which can be explained by four consecutive steps in a full contact-separation cycle, as illustrated in Fig. 3a. Generally, different materials have different affinities for electrons [30]. When considering the rubbing in a variety of materials with each other and seeing the charge transfer between them, the materials can be ordered according to their affinity for electron, which is called as triboelectric series [30–32]. In the triboelectric series, FEP has a greater affinity for electrons than that of paper. In the original state when the two materials contacted (i), the FEP dielectric layer accepting the electrons was negatively charged, while the paper dielectric layer losing the electrons produced positive charges. It should be noted that

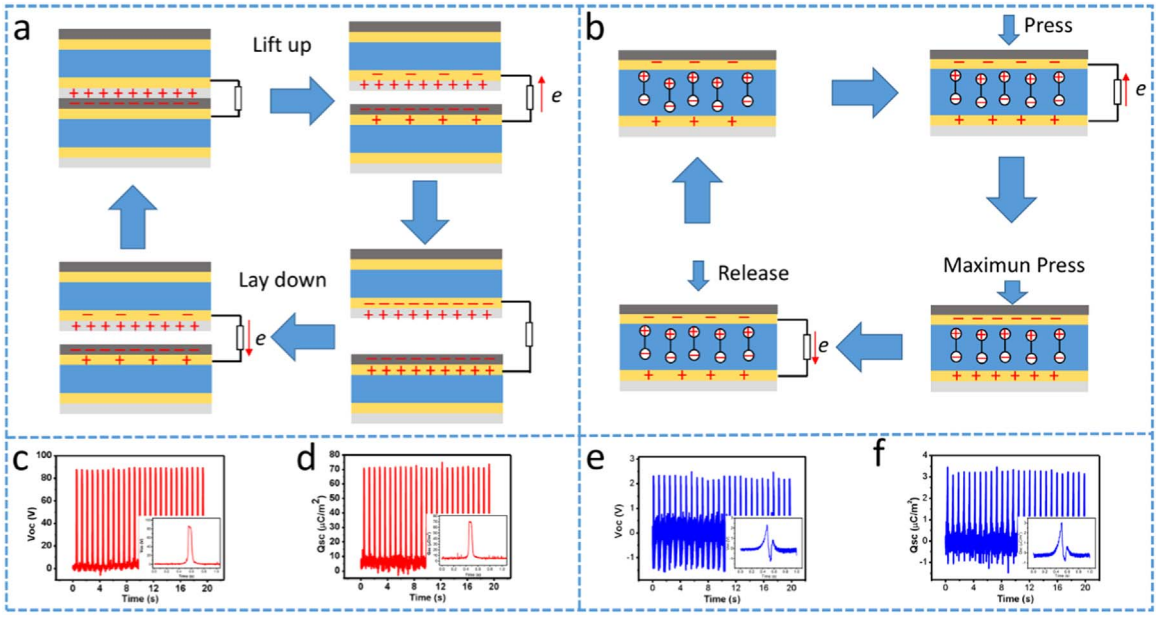

Fig. 3. The working mechanism and electrical performance of the TENG and PENG. The four basic states of one cycle output in (**a**) TENG and (**b**) PENG. (**c**)-(**d**) open-circuit voltage (V_{OC})-time curve and short-circuit charge transfer (Q_{SC})-time curve of TENG. (**e**)-(**f**) V_{OC}-time curve and Q_{SC}-time curve of PENG. Inserts in (**c**)-(**f**) show the enlarged curves of the V_{OC} and Q_{SC}.

the triboelectric charges on the dielectric layer surface will be retained for a long period of time due to the nature of electrets. Once the paper layer begins to separate from the FEP layer (ii), an electric potential difference (EPD) between the two electrodes was created, electrons would flow from the FEP electrode to the paper electrode through the external circuits to balance the electrostatic status. To confirm the existence of the EPD, the finite element method has been utilized to simulate the potential distribution when the distance between the paper and FEP layers varied using COMSOL software. The simulation results of the potential distribution under the open-circuit condition in first three states are shown in Fig. S2a–c. When the full separation was made (iii), an instantaneous balance was achieved and the electrons transfer stopped. As the paper page was laid down, electrons flowed back between the two electrodes through the external circuits to rebalance the electrostatic status (iv). Thus, the alternative current can be produced through periodically flipping the paper pages.

In the PENG part, the piezoelectric effect could be explained by pressing and releasing forces induced by human motions. As illustrated in Fig. 3b, the PVDF nanofibers membrane was fabricated with the polarization direction upward and the original state has no applied force (i). During periodical motions, the PVDF membrane experienced a reciprocating pressing-releasing force resulting in four continuous steps of piezoelectric effects. When the page was laid down, the pressing force was applied on the PVDF membrane, which produced a negative strain and decreased volume. As a result, the polarization density was enhanced and the electron flowed from the bottom electrode to the top electrode to balance the extra polarization density in the short-circuit condition (ii). Here, the finite element method was utilized to simulate the potential distribution induced by variations of the polarization density in PVDF using COMSOL software. The simulation results of the potential distribution under open-circuit condition in first three states are shown in Fig. S2d–f. As the fully contact between two pages was made, the largest pressing force was achieved with the highest polarization density (iii). When the page was lifted, the applied force decreased and then the electron flowed back to rebalance the charge induced by the strain releasing in the short-circuit condition (iv). By reciprocating piezoelectric effects, alternative currents would be produced.

The performance of the TENG and PENG was measured when the paper page was flipped periodically. As shown in Fig. 3c for TENG, the open-circuit voltage (V_{OC}) oscillated with a peak-to-peak value of approximately 90 V (left). In the short-circuit condition, the transfer charges (Q_{SC}) was measured to be an oscillated value with a peak value of about 72 $\mu C/m^{-2}$ (Fig. 3d) and a pulse short-circuit current of about 6 mA/m^2 (Fig. S3a). To confirm the optimized load resistance and the maximum power density outputs, the external loads with different resistances were carried out. Note S1 shows the calculation method of the output power densities. When the load resistance increased, the amplitudes of the output voltage peaks were observed to rise until a saturated value of 89.5 V while the maximum peak power density experienced a different tendency which increased firstly and then gradually dropped with a maximum power density of 285.6 mW/m^2 at the matched load of 2.5 MΩ (Fig. S3b). In the PENG part, there were reciprocating oscillations of about 4 V and 5 $\mu C/m^{-2}$ in the V_{OC} (Fig. 3e) and Q_{SC} (Fig. 3f) with a periodical pulse I_{SC} of about 0.2 mA/m^2 (Fig. S3c), when the motion was applied periodically (Fig. 3d). Moreover, the electrical output performance was observed to gradually rise when the thickness of the PVDF nanofibers membrane increased (Fig. S4). This is because the volume variation of the electrospun PVDF nanofibers membrane raised with increased thickness, which resulted in an enhanced piezoelectric effects. To optimize the output power density produced by the PENG, external load was

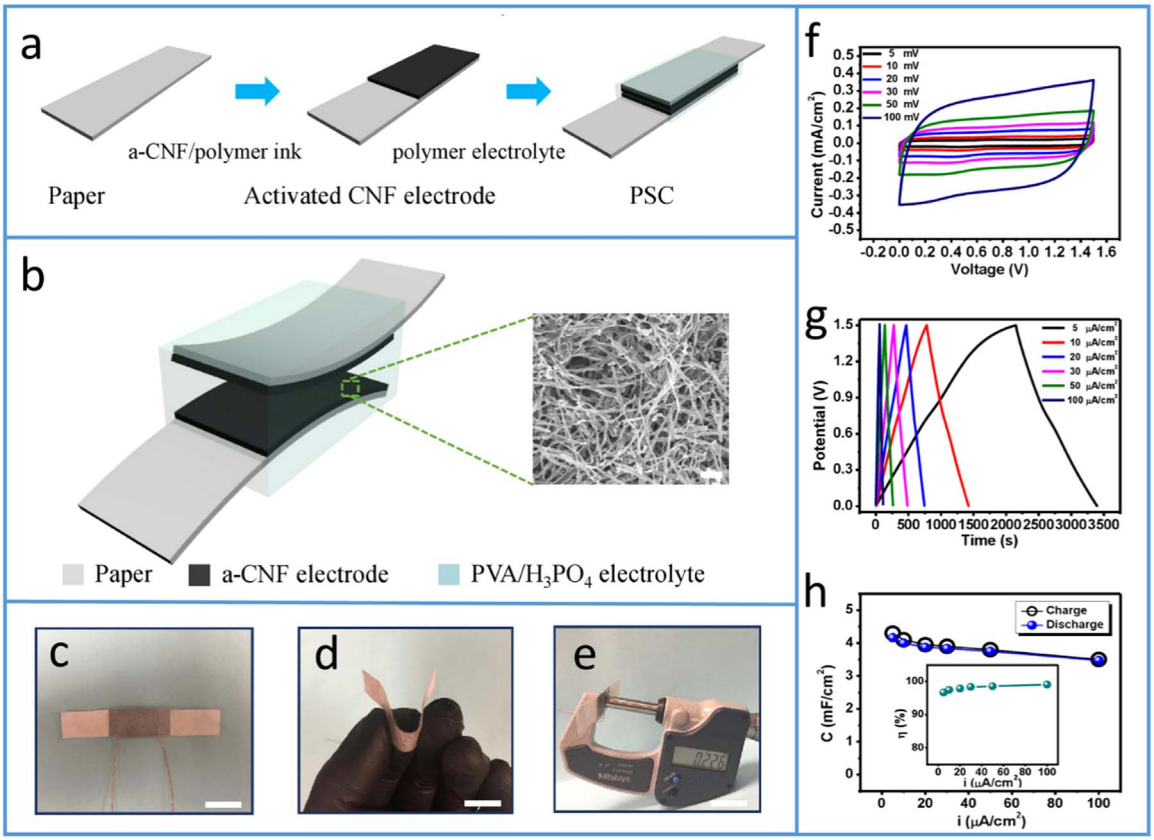

Fig. 4. Fabrication process, schematic and electrochemical performance of the PSC. (**a**) Fabrication process of the PSC. (**b**) Schematic structure of the PSC. Right insert shows the SEM image of the a-CNF/polymer electrode. Scale bar: 1 μm. The photographs of a single PSC, (**c**) original state, and (**d**) bent state, and (**e**) thickness of the PSC. Scale bar: 10 mm. Capacitance properties of a single PSC, (**f**) cyclic voltammetry (CV) curves at various scanning rates, (**g**) galvanostatic charging/dischanging (GCD) curves at different current densities, (**h**) the dependence of charging/discharging specific capacitance on different current densities, insert image shows the charging/discharging efficiency of the PSC.

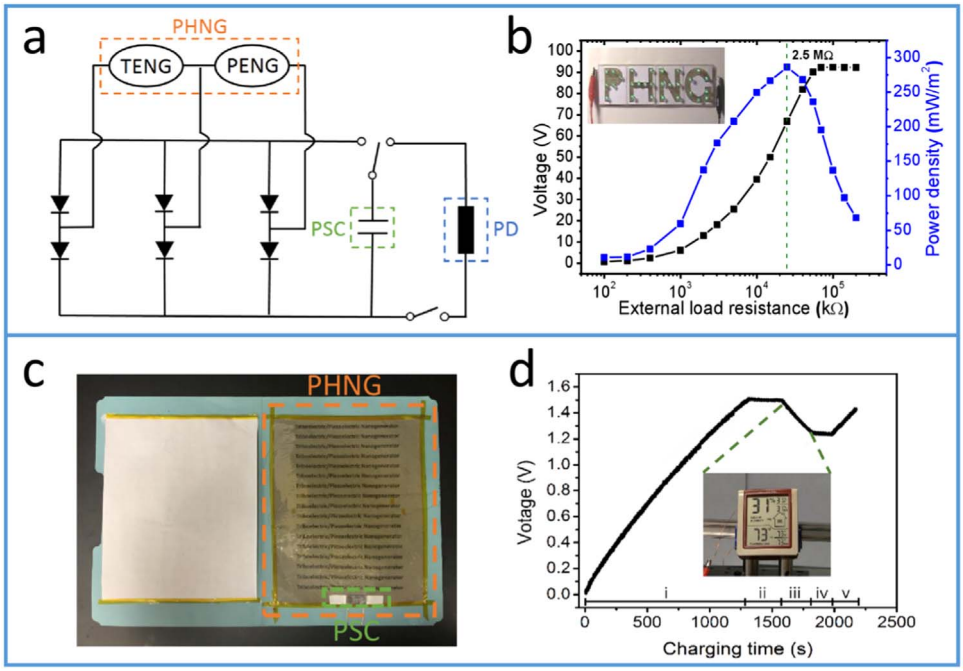

Fig. 5. Power density output and applications of the paper-based self-powered system. (**a**) The electrical circuit of the self-powered system when used as a power source for portable devices (PD). (**b**) Voltage-load resistance and power density-load resistance curves of PHNG, insert shows the photograph when PHNG (2.5 × 2.5 cm^2) was directly used as a power source for lighting up the 28 LEDs. (**c**) Photograph of the PHNG assembled in a book cover. (**d**) The charging curves of the self-powered system under a movement frequency of 2 Hz, and the discharging curve of the self-powered system when it acted as a power source for the working of a temperature/humidity sensor. Insert image shows the temperature/humidity sensor was successfully lighten up by the self-powered system, and the five processes: charging process for i and v, empty loading for ii and iv, discharging process for iii.

applied. As shown in Fig. S3d, the amplitudes of the output voltage peaks were observed to be enhanced as the load resistance increased, while the output power density firstly received a rising trend, following by a decreased tendency, accompanied with a peak power density of 0.65 mW/m^2 at the matched load resistance of 1.8 MΩ. Although the output power of PENG is not as high as that of the TENG, it could serve as a stable and continuous enhancing supplement for energy harvesting through TENG. In order to investigate the stability of the PHNG, continuously working for 10,800 cycles was tested. As shown in Fig. S5, after 10,800 reciprocating cycles, I_{SC} exhibits only negligible drops indicating the high stability and durability of the PHNG.

2.4. Structure design and electrochemical performance of the PSC

Our paper-based solid-state PSC composed of two identical a-CNF (activated carbon nanofibers)/polymer electrodes and H_3PO_4/PVA gel electrolyte, where paper was used as the flexible substrate. Compared with SCs using liquid electrolyte, the all solid state PSC shows advantages such as lightweight, high flexibility, desirable safety and environmental-friendly nature, which are ideal for flexible and portable electronics. To make a thin, flexible and stable SC, a-CNF was chosen as the main material for its highly electrical conductivity, chemical stability and high surface area to volume when used as the electrode [33,34]. In order to achieve a strong adhesion between the paper and a-CNF, a diluted H_3PO_4/PVA gel was chosen to make a composite electrode with a-CNF for the PSC. Here, the diluted H_3PO_4/PVA gel acted as a binder as well as a electrolyte, which not only facilitated the PSC with mechanical flexibility and durability, but also ensured it with excellent electrochemical capacitance properties. The fabrication process and the layered structure of the PSC are schematically illustrated in Fig. 4a and b, respectively. From Fig. 4b, the SEM image of the a-CNF/polymer electrode shows the a-CNF/polymer formed an interconnected micro/nano-porous structure with a high surface area, beneficial for the electrochemical capacitance of the PSC. The photographs of the PSC in normal and bending states are shown in Fig. 4c and d, and it could be observed that the PSC is very thin with a thickness of 226 μm, which is at the same level with that of a paper (Fig. 4c). It has a high flexibility and could be applied in miniaturized electronics.

The electrochemical capacitance properties of PSC were tested by the cyclic voltammetry (CV) method at a series of scanning rate from 5 to 100 mV/s. As illustrated in Fig. 4f, the rectangle-like CV curves indicated our PSC possessed an ideal capacitive behavior and good reversibility. To assess the durability of the PSC during bending, the CV curves of the PSC before and after bent for more than 100 times were tested at a scanning rate of 100 mV/s. From Fig. S6a, the compared capacitances show a 100-bent PSC retained 94.1% capacitance, indicating the PSC has great flexibility and durability. The electrochemical capacitance was further confirmed by galvanostatic charging-discharging (GCD) results at a range of current loads from 5 to 100 mA (Fig. 4g). The classical triangle-shaped charging/discharging curves and an almost identical capacitance were found in all the curves. The voltage was linear in a wide voltage window up to 1.5 V with no obvious ohm-drop phenomenon in GCD analysis at a series of current loads from 5 to 100 $μA/cm^2$. This is mainly attributed to the high electrochemical stability of the carbon nanofibers and solid state electrolyte [33]. The charging/discharging specific capacitance on different current densities could be calculated from GCD curves, and the calculation method was presented in Note S2. As illustrated in Fig. 4h, the area specific capacitance (F/cm^2) decreased when the load current increased while the charging/discharging efficiency (Columbic efficiency, η) increased as the current load increased (insert image in Fig. 4h). Even at a low current of 5 $μA/cm^2$, the PSC could be charged to 1.5 V with an excellent Columbic efficiency of 96.7%, which indicates an extremely low leakage current, enabling its great effectiveness as an energy storage device for energy harvesting with the PHNG. Moreover, it is also crucial to evaluate the cycling stability for supercapacitors. The capacitance has only negligible fluctuation during the cycling test, which changed from the original 4.3 mF/cm^2 to 4.1 mF/cm^2 after 10,000 continuous cycles at a current density of 0.1 mA/cm^2 (Fig. S6b). It was able to maintain as much as 95.3% capacitance, which indicates an excellent cycling performance of the PSC.

2.5. Paper-based self-powered system as a flexible power source

In order to integrate TENG and PENG together for continuously charging the PSC, an optimization of the circuit is designed mainly in the inter-component electrical connection. As illustrated in Fig. 5a, the paper-based TENG and PENG were electrically connected via three pairs of diodes, which served as rectifiers in converting the pulse output signals of the nanogenerators to direct signals for charging the PSC without intermittent. For quantitative characterization, a linear motor with mechanical transmission kit was adopted to mimic various mechanical movements. To optimize the electrical output of the PHNG, a series of external load resistances were employed. As illustrated in Fig. 5b, with the increase of load resistance, the output power density firstly raised and was followed by a drop tendency with a maximum power density of 286.5 mW/m^2 at the optimized load resistance of 2.5 MΩ. This superior value is about 5 times higher than that of previous work on a fiber-based hybrid nanogenerator composed of TENG and PENG [35], and 2 times higher than that of the work on a piezoelectric and triboelectric hybrid nanogenerator [36]. Although the output of PHNG is not higher than the work on Piezo/Triboelectric hybrid generator [37], this work shows an ultrathin, lightweight, flexible, cost-efficiency and transparent hybrid nanogenerator which largely improved the portability and functionality of the PHNG, ensuring more possible applications, such as smart reading and documents management. Different from the output power density, the output voltage was constantly increased and saturated until the load resistance increased by a certain value. To assess the energy harvesting potential in practical applications, the PHNG was firstly used as a direct power source, 28 LEDs were successfully lighten up by the PHNG (2.5 × 2.5 cm^2) with continuous contact-separation movements triggered by hand motions (Video S1). Insert image in up-left corner of Fig. 5b shows the photograph of the lighten LEDs, which were arranged as 'PHNG' characters.

Supplementary material related to this article can be found online at doi:10.1016/j.nanoen.2017.06.046.

To demonstrate the capability of the paper-based self-powered system as a flexible and sustainable power source for practical applications, the paper-based self-powered system was developed by integrating a PHNG (A4 in paper size) with the PSC in a book cover as one page of a book, and an ITO deposited paper as another page (Fig. 5c). Fig. 5d shows the charging/discharging curve of the self-powered device, which demonstrated the paper-based self-powered system could be charged to 1.5 V within 25 min under a moving frequency of 2 Hz. When used as a sustainable power source for the working of a temperature/humidity sensor, the self-powered system discharged at a load current of about 2.5 μA, insert image shows the photograph when temperature/humidity sensor was successfully lighten up by the self-powered system. Realized by the reciprocating movements of the linear motor (Video S2), the self-powered system successfully supported the continuous working of the temperature/humidity sensor after 20-min unremitting charging. To confirm the I_{SC} dependence on different frequencies of moving motions, the charging properties of the self-powered system were tested at a range of low frequencies from 1 to 3 Hz. As illustrated in Fig. S7, the charging time was largely enhanced by increasing the applied moving frequencies.

Supplementary material related to this article can be found online at doi:10.1016/j.nanoen.2017.06.046.

2.6. Paper-based self-powered system for wireless sensing system

To further demonstrate the capability of the paper-based device as a practical self-powered sensor for human-machine interaction, a wireless sensing system was developed by integrating the paper-based TENG in the single-electrode mode with a signal-processing circuit (ARDUINO, UNO R3), as shown in Fig. 6a. The wireless sensing system could be easily operated by the output voltage generated from the TENG (finger/paper touch) to trigger the integrated circuit to produce an infrared signal (IR signal). This remote IR signal then triggered a signal processor, which was connected with the computer though a wireless IR sensor to produce a signal recognition process.

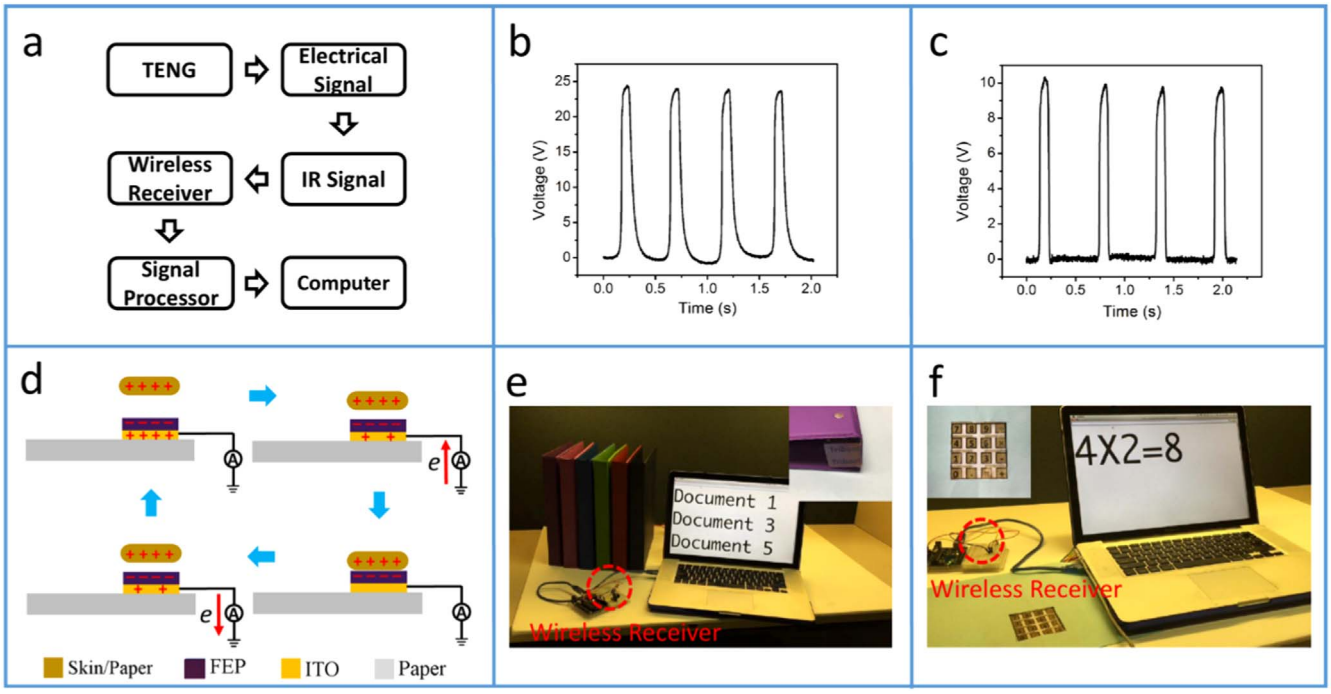

Fig. 6. Self-powered sensing applications of the single electrode TENG. (**a**) Design and schematic of the self-powered sensing system. V_{OC}-time curve of the single electrode TENG, (**b**) reciprocating lift-up and lay-down movements between TENG and paper, (**c**) reciprocating touch and separation motions between TENG and finger. (**d**) The work mechanism of the single electrode TENG triggered by finger/paper touch motions. (**e**) Photograph of the book management system realized by documents moving. Insert image shows the photograph of PHNG assembled on the bottom side of the document, document number: 1–6 from left to right. (**f**) Photograph of the paper-based calculator functionally triggered by finger touch motions. Insert image shows the photograph of the paper-based finger touch calculator.

The output voltage of the single-electrode paper-based TENG (2.5 × 2.5 cm^2) triggered by paper/finger touch motions was shown in Fig. 6b and c, which indicates the output voltages are approximately 25 and 10 V, respectively. Fig. 6d shows the working mechanism of the single electrode realized by paper/finger touch. Since both paper and finger are much more triboelectrically positive than FEP [31,32], to balance the EPD produced between FEP and paper/finger, electrons flowed from ground to the FEP electrode with a touch movement while electrons flowed back with a separation movement.

Through the signal-processing circuit, we developed a wireless human-machine interaction system for documents management, which was firstly realized by moving documents (Fig. 6e). Insert image in the up-right corner shows the photograph of paper-based TENG assembled on the bottom side of the document. As shown in the Video S3, when we moved the document, voltage will be produced by separation movement between paper and FEP, which then triggered the remote controller and IR sensor. Through the signal processor, the relative document number was displayed on the monitor, enabling the management of the documents. It is worthy note that our wireless document management system used a self-powered paper-based TENG which was ultrathin and lightweight enough with advantages of cost-efficiency, environmental friendly and versatility, indicating great potential for applications where mechanical movement could be employed to trigger a signal processing. To further evaluate its potential in human-machine interaction, we developed a smart calculation system. As shown in Fig. 6f, a paper-based calculator was fabricated by using 16 separated square TENGs as the functional keys (insert image in up-left corner). From Video S4, we can observe the corresponding numbers and operative symbols were entered and displayed on the monitor when we touched the relevant functional keys, and the mathematical operation was carried out when we touched the equal sign. Another video demonstration for smart reading was illustrated by line recording (Video S5), the computer helped us keep a record of the line number we have read in a simply way by using finger to touch the relevant line. Furthermore, the effective working ability of the device on different distance was evaluated, and the effective distance for triggering the circuit was found to be within 6 m.

Supplementary material related to this article can be found online at doi:10.1016/j.nanoen.2017.06.046.

3. Conclusion

In summary, we have presented an ultrathin, lightweight, flexible, and sustainable self-powered system by fabricating a hybrid nanogenerator with an all-solid-state supercapacitor in a thin paper. Based on the bottom-up method and electrospinning technique, the reported paper-based self-powered system introduces a simple and versatile strategy with greatly reduced device thickness, lightweight and suitability for mass production. Possessing an ultrathin multi-layered structure with a thickness of ~200 μm, the self-powered system was highly deformable without sacrificing the readability of the paper and easily to be assembled in books and documents. Under human motions such as flipping pages, moving book/document, the as-fabricated smart book/document was capable of being a sustainable power source for practical applications, including continuously powering LEDs and the temperature/humidity sensor. Through the signal-processing circuit, the paper-based system was further developed into a wireless human-machine interaction system which is cost-efficient, environmental-friendly and versatile for documents management and smart reading via the single-electrode mode of TENG. The paper-based self-powered system could be extensively applied not only as sustainable power source for self-powered electronics but also possibly as self-powered sensors for broad applications in the IoT.

4. Experimental methods

4.1. Fabrication of the PHNG

Copy paper was selected as the starting material and deposited with a thin ITO layer by PVD. For ITO deposition process, power supply was set to 100 W, capman pressure for argon was set to 6 mTorr, and the deposition time was 20 min. PVDF solution (23%) was prepared by dissolving 2.3 g PVDF pellets (Mw 180,000 by GPC, Sigma-Aldrich) in 10 mL solvent mixture of dimethylformamide (Sigma-Aldrich) and acetone (Sigma-Aldrich) (volume ratio of dimethylformamide and acetone, 5/5) and heated at 70 °C for 2 h. The ITO deposited paper was directly used as collector in the electrospinning process for fabricating an ultrathin PVDF nanofibers membrane (thickness varies from different electrospinning time, generally a thickness of about 20 μm can be formed in an hour) on the paper. During the electrospinning process, voltage of 18 kV, tip-to-collector of 15 cm, and flow rate of 3 mL/h were applied. Then, the liquid PDMS (Sylgard 184, Dow Corning, the mixed mass ratio of PDMS and the curing agent is 10:1) was degassed for 1 h and dropped onto the PVDF nanofibers membrane until the liquid PDMS fully penetrated throughout the PVDF membrane to become a transparent PDMS/PVDF composite membrane. After that, the surface of the FEP film (25 μm) was fabricated with a nanowires array structure via inductively coupled plasma (ICP) reactive-ion etching [28], and with a thin ITO layer deposited on another side of the FEP. The ITO side was sequentially assembled on top of the composite membrane by slightly compressing. Finally, the as-fabricated PHNG was dried at 50 °C in the oven for 16 h.

4.2. Fabrication of the PSC

The PVA/H_3PO_4 gel electrolyte was prepared as follows: 10 g of H_3PO_4 (85% aq. soln., Alfa Aesar) was added into 100 mL of deionized water, and then 10 g of PVA (Mw 89,000–98,000, 99+% hydrolyzed, Sigma-Aldrich) powder. The mixture was heated to 85 °C under stirring until the solution became clear. The a-CNF/polymer electrode was prepared by drop-casting a desirable amount of a-CNF/polymer ink onto the paper and oven dried at 75 °C for 2 h. Typically, to prepare the a-CNF/polymer ink, 0.4 g a-CNF (PR-24-XT-HHT, Pyrograf Products, Inc.) was added in 100 mL diluted PVA/H_3PO_4 (10 times diluted by deionized water) solution, follow by a sonication and stirring process. The prepared electrodes were immersed into PVA/H_3PO_4 solution for 10 min, with their two-end parts kept above the solution. After being taken out, every two electrodes were face-to-face assembled with a thin PVA/H_3PO_4 membrane in between, leaving aside the bare part as the electrode terminal. Here, the PVA/H3PO4 membrane served as an insulator as well as the electrolyte for the PSC, which helped reduce the weight and thickness of the device. When the PVA/H_3PO_4 gel solidified at room temperature, the flexible PSC was obtained. Normally, the PSC with an area of 2 cm^2 was fabricated and used in the study.

4.3. Characterization and measurements

A Hitachi SU8010 field emission SEM was used to measure the morphology and size of the a-CNF/polymer electrode, electrospun PVDF nanofibers membrane and FEP nanowires array. A potentiostat (Princiton Application Research) was utilized to test the capacitance properties by using CV and GCD techniques. For the electric output measurement of the TENG/PENG, a commercial linear motor was applied to drive the TENG/PENG contact and separate, and a programmable electrometer (Keithley, model 6514) was adopted to test the electrical output performances. For stably testing, the gap between layers is set to 10 mm. The thickness of the devices was measured by an electronic digital micrometer (733 Series Electronic Digital Micrometers, L.S. Starrett).

Acknowledgements

X.H., Y.Z. and H.Y. contributed equally to this work. This research was supported by the Hightower Chair foundation and the 'thousands talents' programme for pioneer researcher and his innovation team, China, National Natural Science Foundation of China (Grant nos. 51432005 and 51473100), State Key Laboratory of Polymer Materials Engineering (sklpme2016-3-09), Excellent Young Scholar Fund of Sichuan University (2015SCU04A26), and Chongqing Research Program of Basic Research and Frontier Technology (Grant nos. CSTC2014jcyjA40032 and CSTC2015jcyjA40017). X.H. thanks the China Scholarship Council for supporting research at the Georgia Institute of Technology, USA.

Appendix A. Supporting information

Supplementary data associated with this article can be found in the online version at doi:10.1016/j.nanoen.2017.06.046.

References

[1] Z.L. Wang, Mater. Today (2017).
[2] Z.L. Wang, J. Chen, L. Lin, Energy Environ. Sci. 8 (2015) 2250–2282.
[3] Z.L. Wang, J. Song, Science 312 (2006) 242–246.
[4] M. Lee, C.Y. Chen, S. Wang, S.N. Cha, Y.J. Park, J.M. Kim, L.J. Chou, Z.L. Wang, Adv. Mater. 24 (2012) 1759–1764.
[5] F.-R. Fan, Z.-Q. Tian, Z.L. Wang, Nano Energy 1 (2012) 328–334.
[6] Y. Yang, Y. Zhou, J.M. Wu, Z.L. Wang, ACS Nano 6 (2012) 8456–8461.
[7] Z.L. Wang, Faraday Discuss. 176 (2015) 447–458.
[8] D. Pech, M. Brunet, H. Durou, P. Huang, V. Mochalin, Y. Gogotsi, P.-L. Taberna, P. Simon, Nat. Nanotechnol. 5 (2010) 651–654.
[9] J. Wang, X. Li, Y. Zi, S. Wang, Z. Li, L. Zheng, F. Yi, S. Li, Z.L. Wang, Adv. Mater. 27 (2015) 4830–4836.
[10] Y. Zi, J. Wang, S. Wang, S. Li, Z. Wen, H. Guo, Z.L. Wang, Nat. Commun. 7 (2016).
[11] Z. Wen, M.-H. Yeh, H. Guo, J. Wang, Y. Zi, W. Xu, J. Deng, L. Zhu, X. Wang, C. Hu, Sci. Adv. 2 (2016) e1600097.
[12] F.-R. Fan, L. Lin, G. Zhu, W. Wu, R. Zhang, Z.L. Wang, Nano Lett. 12 (2012) 3109–3114.
[13] S. Kim, M.K. Gupta, K.Y. Lee, A. Sohn, T.Y. Kim, K.S. Shin, D. Kim, S.K. Kim, K.H. Lee, H.J. Shin, Adv. Mater. 26 (2014) 3918–3925.
[14] J. Luo, W. Tang, F.R. Fan, C. Liu, Y. Pang, G. Cao, Z.L. Wang, ACS Nano 10 (2016) 8078–8086.
[15] Y.H. Jung, T.-H. Chang, H. Zhang, C. Yao, Q. Zheng, V.W. Yang, H. Mi, M. Kim, S.J. Cho, D.-W. Park, Nat. Commun. 6 (2015).
[16] F. Eder, H. Klauk, M. Halik, U. Zschieschang, G. Schmid, C. Dehm, Appl. Phys. Lett. 84 (2004) 2673–2675.
[17] X. Liu, M. Mwangi, X. Li, M. O'Brien, G.M. Whitesides, Lab Chip 11 (2011) 2189–2196.
[18] F. Güder, A. Ainla, J. Redston, B. Mosadegh, A. Glavan, T. Martin, G.M. Whitesides, Angew. Chem. 128 (2016) 5821–5826.
[19] J.T. Overvelde, T.A. De Jong, Y. Shevchenko, S.A. Becerra, G.M. Whitesides, J.C. Weaver, C. Hoberman, K. Bertoldi, Nat. Commun. 7 (2016).
[20] J. Liu, C. Yang, H. Wu, Z. Lin, Z. Zhang, R. Wang, B. Li, F. Kang, L. Shi, C.P. Wong, Energy Environ. Sci. 7 (2014) 3674–3682.
[21] X. Fan, J. Chen, J. Yang, P. Bai, Z. Li, Z.L. Wang, ACS Nano 9 (2015) 4236–4243.
[22] C. Wu, X. Wang, L. Lin, H. Guo, Z.L. Wang, ACS Nano 10 (2016) 4652–4659.
[23] H. Guo, M.-H. Yeh, Y.-C. Lai, Y. Zi, C. Wu, Z. Wen, C. Hu, Z.L. Wang, ACS Nano 10 (2016) 10580–10588.
[24] A. Chandrasekhar, N.R. Alluri, B. Saravanakumar, S. Selvarajan, S.-J. Kim, ACS Appl. Mater. Interfaces 8 (2016) 9692–9699.
[25] A. Chandrasekhar, N.R. Alluri, V. Vivekananthan, Y. Purusothaman, S.-J. Kim, J. Mater. Chem. C (2017).
[26] J. Fang, X. Wang, T. Lin, J. Mater. Chem. 21 (2011) 11088–11091.
[27] C. Lang, J. Fang, H. Shao, X. Ding, T. Lin, Nat. Commun. 7 (2016).
[28] J. Chen, G. Zhu, J. Yang, Q. Jing, P. Bai, W. Yang, X. Qi, Y. Su, Z.L. Wang, ACS Nano 9 (2015) 105–116.
[29] Y. Zi, L. Lin, J. Wang, S. Wang, J. Chen, X. Fan, P.K. Yang, F. Yi, Z.L. Wang, Adv. Mater. 27 (2015) 2340–2347.
[30] J.W. Lee, B.U. Ye, J.M. Baik, APL Mater. 5 (2017) 073802.
[31] A. Diaz, R. Felix-Navarro, J. Electrost. 62 (2004) 277–290.
[32] W. Yang, J. Chen, G. Zhu, J. Yang, P. Bai, Y. Su, Q. Jing, X. Cao, Z.L. Wang, ACS Nano 7 (2013) 11317–11324.
[33] Z.S. Wu, A. Winter, L. Chen, Y. Sun, A. Turchanin, X. Feng, K. Müllen, Adv. Mater. 24 (2012) 5130–5135.
[34] L.-F. Chen, Z.-H. Huang, H.-W. Liang, W.-T. Yao, Z.-Y. Yu, S.-H. Yu, Energy Environ. Sci. 6 (2013) 3331–3338.
[35] X. Li, Z.-H. Lin, G. Cheng, X. Wen, Y. Liu, S. Niu, Z.L. Wang, ACS Nano 8 (2014) 10674–10681.
[36] B. Shi, Q. Zheng, W. Jiang, L. Yan, X. Wang, H. Liu, Y. Yao, Z. Li, Z.L. Wang, Adv. Mater. 28 (2016) 846–852.
[37] W.-S. Jung, M.-G. Kang, H.G. Moon, S.-H. Baek, S.-J. Yoon, Z.-L. Wang, S.-W. Kim, C.-Y. Kang, Sci. Rep. 5 (2015) 9309.

Xu He received his B.S. in Polymer Materials and Engineering from Sichuan University (SCU, China, 2006–2010) and MSc in Materials Science from SCU (2011–2014). He started to pursue his Ph.D. degree in Materials Science at SCU in 2014. Now he is a visiting Ph.D. student in Materials Science and Engineering at Georgia Institute of Technology through the program of China Scholarship Council (CSC). His research focuses primarily on nanocellulose/functional polymer materials fabrication, nanomaterial-based energy harvesting/storage, active sensing and self-powered micro-/nano-systems.

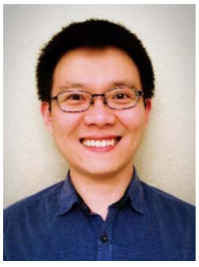

Dr. Yunlong Zi received his Bachelor of Engineering from Department of Materials Science and Engineering at Tsinghua University, Beijing, China, in 2009, and his Ph.D. from Department of Physics at Purdue University, West Lafayette, Indiana, USA, in 2014. He is currently working as a post-doctoral fellow at Georgia Institute of Technology under supervision of Prof. Zhong Lin Wang. His research interests include fundamental physics of triboelectric nanogenerators, hybrid nanogenerator for energy harvesting, self-powered systems, nanoelectronics and synthesis of semiconductor nanomaterials. As the 1st authors, his research have been published in top journals, including Nature Nanotechnology, Nature Communications, Advanced Materials, Nano Letters and etc. He was honored as the winner of MRS Postdoctoral Award by Materials Research Society in 2017, as the first recipient from Georgia Tech; and one of "5 students who are transformation makers" by Purdue University in 2013, as highlighted in Purdue homepage.

Hua Yu received his Ph.D in 2006 from Huazhong University of Science & Technology, China. He is currently a professor in Chongqing University, China. His main research interests focus on the MEMS, energy harvesting, IC design and self-powered sensor.

Steven Zhang received his B.S. degree in Electronic Materials Engineering from U.C. Davis in 2014. He is currently pursuing a Ph.D. in Material Science and Engineering at Georgia Institute of Technology, and is working for Dr. Zhong Lin Wang. His research focused on nanogenerators, energy harvesting, and self-powered active sensing.

Dr. Jie Wang is currently a professor at Beijing Institute of Nanoenergy and Nanosystems, Chinese Academy of Sciences. His main research interests focus on the energy materials, self-powered system, supercapacitors and nanogenerators.

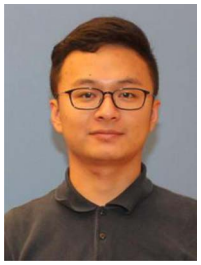

Dr. Wenbo Ding received the B.E and Ph.D. degrees (both with the highest honors) from the Department of Electronic Engineering, Tsinghua University, Beijing, China, in 2011 and 2016, respectively. He is now a postdoctoral research fellow in Materials Science and Engineering at Georgia Tech, Atlanta, GA, working with Professor Z. L. Wang. His research interests include self-powered sensors, energy harvesting, soft robotics, human-machine interface with the help of signal processing and machine learning. He has received many prestigious awards, including the IEEE Scott Helt Memorial Award, the best paper award of the National Doctoral Student Academic Conference, the Tsinghua Top Grade Scholarship (highest honor in Tsinghua), the Excellent Ph.D. Graduate of Beijing City, and the Excellent Doctoral Dissertation of Tsinghua University.

Haiyang Zou received his M.S. degree in Worcester Polytechnic Institute, United States in 2012 and B.S. degree in Nanchang University, China in 2010. He is currently a Ph.D. candidate in Georgia Institute of Technology under the supervision of Prof. Zhong Lin Wang. Haiyang's research interests include energy nano-materials, nano-systems and nano-devices; peizoelectro-nics and piezo-optoelectronics, flexible electronics.

Wei Zhang is an associate professor in the State Key Lab of Polymer Materials Engineering at Sichuan University (SCU), China. He received his Ph.D. in 2012 in Materials Science from SCU. He was a visiting scholar in Materials Science and Engineering at Georgia Institute of Technology during 2009–2011. He is a member of Technical Association of the Pulp and Paper Industry (TAPPI), Chinese Chemical Society, Biomedical Materials Association of China. His research interests focus on nanocellulose materials, ultra-strong UHMWPE fibers, functional polymer materials and flexible electrical devices.

Canhui Lu is a professor in the State Key Lab of Polymer Materials Engineering at Sichuan University (SCU), China. He received his Ph.D. in Materials Science from SCU in 2002. He is the deputy secretary-general of the expert committee of China Plastics Processing Industry Association and the deputy secretary-general of Sichuan Tire Renovation and Utilization Association. He was awarded the Outstanding Expert of Sichuan Province in 2006. His research was awarded the second prize of the National Technological Invention Award in 2006, the first prize of the Technological Invention of the Ministry of Education in 2002 and the Golden Medal of Chinese Patent in 2017. His research interests include polymer composites and polymer chemistry, ultrafine particles, recycling and utilization of waste polymer materials, functional polymer materials and flexible electronic devices.

Zhong Lin (ZL) Wang received his Ph.D. from Arizona State University in physics. He now is the Hightower Chair in Materials Science and Engineering, Regents' Professor, Engineering Distinguished Professor and Director, Center for Nanostructure Characterization, at Georgia Tech. Dr. Wang has made original and innovative contributions to the synthesis, discovery, characterization and understanding of fundamental physical properties of oxide nanobelts and nanowires, as well as applications of nanowires in energy sciences, electronics, optoelectronics and biological science. His discovery and breakthroughs in developing nanogenerators established the principle and technological road map for harvesting mechanical energy from environment and biological systems for powering personal electronics. His research on self-powered nanosystems has inspired the worldwide effort in academia and industry for studying energy for micro-nano-systems, which is now a distinct disciplinary in energy research and future sensor networks. He coined and pioneered the field of piezotronics and piezo-phototronics by introducing piezoelectric potential gated charge transport process in fabricating new electronic and optoelectronic devices. Details can be found at: http://www.nanoscience.gatech.edu.